Time Evolution of the Kondo Resonance in Response to a Quench

H. T. M. Nghiem and T. A. Costi

Time evolution of the Kondo resonance in response to a quench

H. T. M. Nghiem[1,2] and T. A. Costi[1]

[1]*Peter Grünberg Institut and Institute for Advanced Simulation, Research Centre Jülich, 52425 Jülich, Germany*
[2]*Advanced Institute for Science and Technology, Hanoi University of Science and Technology, 10000 Hanoi, Vietnam*

We investigate the time evolution of the Kondo resonance in response to a quench by applying the time-dependent numerical renormalization group (TDNRG) approach to the Anderson impurity model in the strong correlation limit. For this purpose, we derive within TDNRG a numerically tractable expression for the retarded two-time nonequilibrium Green function $G(t + t', t)$, and its associated time-dependent spectral function, $A(\omega, t)$, for times t both before and after the quench. Quenches from both mixed valence and Kondo correlated initial states to Kondo correlated final states are considered. For both cases, we find that the Kondo resonance in the zero temperature spectral function, a preformed version of which is evident at very short times $t \to 0^+$, only fully develops at very long times $t \gtrsim 1/T_K$, where T_K is the Kondo temperature of the final state. In contrast, the final state satellite peaks develop on a fast time scale $1/\Gamma$ during the time interval $-1/\Gamma \lesssim t \lesssim +1/\Gamma$, where Γ is the hybridization strength. Initial and final state spectral functions are recovered in the limits $t \to -\infty$ and $t \to +\infty$, respectively. Our formulation of two-time nonequilibrium Green functions within TDNRG provides a first step towards using this method as an impurity solver within nonequilibrium dynamical mean field theory.

Introduction.— The nonequilibrium properties of strongly correlated quantum impurity models continue to pose a major theoretical challenge. This contrasts with their equilibrium properties, which are largely well understood [1], or can be investigated within a number of highly accurate methods, such as the numerical renormalization group method (NRG) [2–5], the continuous time quantum Monte Carlo (CTQMC) approach [6], the density matrix renormalization group [7], or the Bethe ansatz method [8, 9]. Quantum impurity models far from equilibrium are of direct relevance to several fields of research, including charge transfer effects in low-energy ion-surface scattering [10–17], transient and steady state effects in molecular and semiconductor quantum dots [18–36], and also in the context of dynamical mean field theory (DMFT) of strongly correlated lattice models [37–39], as generalized to nonequilibrium [40–42]. In the latter, further progress hinges on an accurate non-perturbative solution for the nonequilibrium Green functions of an effective quantum impurity model. Such a solution, beyond allowing time-resolved spectroscopies of correlated lattice systems within DMFT to be addressed [43–47], would also be useful in understanding time-resolved scanning tunnelling microscopy of nanoscale systems [48] and proposed cold atom realizations of Kondo correlated states [49–52], which could be probed with real-time radio-frequency spectroscopy [53–55].

In this Letter, we use the time-dependent numerical renormalization group (TDNRG) approach [56–62] to calculate the retarded two-time Green function, $G(t_1 = t + t', t_2 = t)$, and associated spectral function, $A(\omega, t)$, of the Anderson impurity model in response to a quench at time $t = 0$, and apply this to investigate in detail the time evolution of the Kondo resonance. This topic has been addressed before within several approaches, including the non-crossing approximation [26, 63], conserving approximations [64] and within CTQMC for quantum dots out of equilibrium [32]. Related work on the temporal evolution of the spin-spin correlation function

in the Kondo model and thermalization in the Anderson impurity model following initial state preparations has also been carried out [65, 66]. Formulations of the time-dependent spectral function within TDNRG are also available [59, 67], but only for positive times. Here, we derive expressions for the two-time Green function and spectral function $A(\omega, t)$ which are numerically tractable at arbitrary times, including negative times. The main advantages of the TDNRG over other approaches for calculating time-dependent spectral functions is that it can access arbitrary long times ($t \to \pm\infty$) and arbitrary low temperatures and frequencies, is non-perturbative and calculates spectral functions directly on the real frequency axis. It is therefore well suited for investigating the formation in time of the exponentially narrow and low temperature Kondo resonance [68]

Model and quenches.—We consider the time-dependent Anderson impurity model, $H = \sum_\sigma \varepsilon_d(t) n_{d\sigma} + U(t) n_{d\uparrow} n_{d\downarrow} + \sum_{k\sigma} \epsilon_k c_{k\sigma}^\dagger c_{k\sigma} + \sum_{k\sigma} V(c_{k\sigma}^\dagger d_\sigma + d_\sigma^\dagger c_{k\sigma})$, where $\varepsilon_d(t) = \theta(-t)\varepsilon_i + \theta(t)\varepsilon_f$ is the energy of the local level, $U(t) = \theta(-t)U_i + \theta(t)U_f$ is the local Coulomb interaction, σ labels the spin, $n_{d\sigma} = d_\sigma^\dagger d_\sigma$ is the number operator for local electrons with spin σ, and ε_k is the kinetic energy of the conduction electrons with constant density of states $\rho(\omega) = \sum_k \delta(\omega - \varepsilon_k) = 1/2D$ with $D = 1$ the half-bandwidth. We take $\Gamma \equiv \pi\rho(0)V^2 = 0.001$ throughout and consider two types of quench [referred to subsequently as quench (A) or quench (B)]: (A), from a symmetric Kondo regime with $\varepsilon_i = -15\Gamma, U_i = 30\Gamma$ and a vanishingly small Kondo scale $T_K^i = 3 \times 10^{-8}$ [69] to a symmetric Kondo regime with $\varepsilon_f = -6\Gamma, U_f = 12\Gamma$ and a larger Kondo scale $T_K = 2.5 \times 10^{-5}$, and, (B), from a mixed valence regime with $\varepsilon_i = -\Gamma, U_i = 8\Gamma$ to a symmetric Kondo regime with $\varepsilon_f = -4\Gamma, U_f = 8\Gamma$ and a Kondo scale $T_K = 1.0 \times 10^{-4}$.

Spectral function $A(\omega, t)$.— We obtain the time-dependent spectral function via $A(\omega, t) = -\frac{1}{\pi}\text{Im}[G(\omega + i\eta, t)]$, where $G(\omega + i\eta, t)$, with infinitesimal $\eta > 0$, is the Fourier transform of $G(t + t', t) \equiv -i\theta(t')\langle[d_\sigma(t + t'), d_\sigma^\dagger(t)]_+\rangle_{\hat{\rho}}$ with respect

to the relative time t' and $\hat{\rho}$ denotes the full density matrix of the initial state [70–72]. In the notation of Ref. 61, we find for the case of positive times [73]

$$G(\omega + i\eta, t) = \sum_{m=m_0}^{N} \sum_{rsq}^{\notin KK'K''} \rho_{sr}^{i\to f}(m) e^{-i(E_s^m - E_r^m)t}$$

$$\times \left(\frac{B_{rq}^m C_{qs}^m}{\omega + E_r^m - E_q^m + i\eta} + \frac{C_{rq}^m B_{qs}^m}{\omega + E_q^m - E_s^m + i\eta} \right), \quad (1)$$

where $B = d_\sigma$, $C = d_\sigma^\dagger$, and $\rho_{sr}^{i\to f}(m) = \sum_{e\ f}\langle sem|\hat{\rho}|rem\rangle_f$ is the full reduced density matrix projected onto the final states [61]. A somewhat more complicated expression can be derived for negative times [73]. From Eq. (1), we see that the spectral function can be calculated highly efficiently at all times and frequencies from a knowledge of $\rho_{sr}^{i\to f}(m)$, the final state matrix elements, and excitations at each shell m. Our expressions for $A(\omega, t)$ in the two time domains $t < 0$ and $t > 0$ recover the initial and final state spectral functions for $t \to -\infty$ and $t \to +\infty$, respectively and satisfy the spectral sum rule $\int_{-\infty}^{+\infty} d\omega A(\omega, t) = 1$ exactly [73]. Below, we shall first focus on positive times, where the main time evolution of the Kondo resonance occurs, then on negative to positive times, showing how the high energy final state features in $A(\omega, t)$ evolve from their initial state counterparts already at negative times.

Results for positive times.— Consider quench (A), i.e., switching between symmetric Kondo regimes with $T_K^i \ll T_K$. Figure 1(a) shows the overall time-dependence of the spectral function $A(\omega > 0, t > 0) = A(-\omega, t > 0)$. Two structures, associated with two energy scales, are visible at all times $t > 0$: the satellite peak at $\omega = \varepsilon_f + U_f \approx 240 T_K$ and a structure on the scale of T_K around the Fermi level. The former has negligible time-dependence, indicating that the satellite peak in the spectral function has already formed by time $t = 0$ (its evolution at negative times from the initial state satellite peak at $\omega = \varepsilon_i + U_i > \varepsilon_f + U_f$ is discussed below). In contrast to this, the structure around the Fermi level has significant time-dependence at $t > 0$ and evolves into the fully formed final state Kondo resonance only on time scales $t \gtrsim 1/T_K$ [Figs. 1(c) and 1(d)] in agreement with Ref. 26 for the $U = \infty$ Anderson model. For $tT_K \gg 1$, the height of the Kondo resonance at the Fermi level approaches its unitary value given by the Friedel sum rule $\pi\Gamma A(\omega = 0, t \to \infty) = 1$ to within 15% [Fig. 1(d)]. The small deviation from the expected value is a result of incomplete thermalization due to the discretized Wilson chain used within TDNRG [67, 73, 76]. Consequently, evaluating $A(\omega, t \to \infty)$ via the self-energy [77] does not improve the Friedel sum rule further in this limit [59]. In the opposite limit, $t \to -\infty$, where thermalization is not an issue, we recover the Friedel sum rule to within 3% (discussed below). The use of a discrete Wilson chain is also the origin of the small substructures at $|\omega| \lesssim T_K$ in Figs. 1(b)-1(d), effects seen in the time evolution of other quantities, such as the local occupation, and explained in terms of the discrete Wilson chain [78]. On shorter time scales, $tT_K \lesssim 1$, states in the region $T_K^i \ll |\omega| < T_K$, initially missing [Fig. 1(b)], are
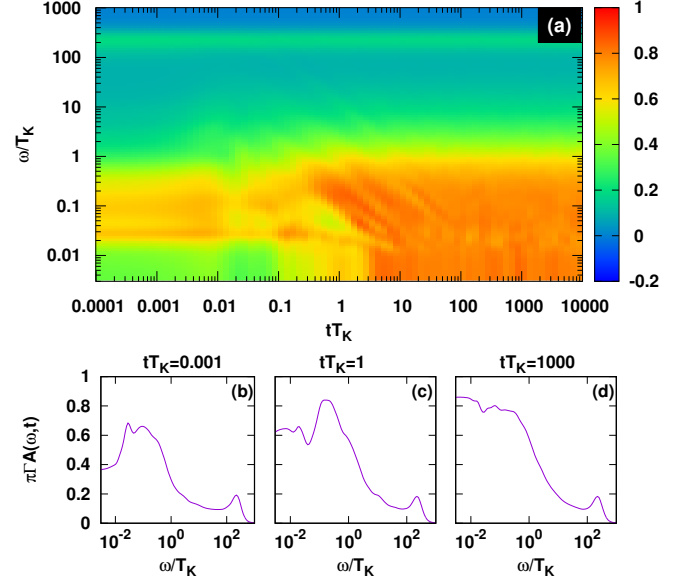

FIG. 1. (a) Time evolution of the normalized spectral function $\pi\Gamma A(\omega > 0, t)$ for the symmetric Anderson model at positive times, following a quench at $t = 0$ specified by $\varepsilon_i = -15\Gamma$, $U_i = 30\Gamma$ and $\varepsilon_f = -6\Gamma$, $U_f = 12\Gamma$ with final state Kondo temperature $T_K = 2.5 \times 10^{-5}$. A structure on the scale of T_K evolves into the Kondo resonance at long times $t \gtrsim 1/T_K$, while a structure at $\omega = \varepsilon_f + U_f \approx 240 T_K$ with negligible time-dependence corresponds to the final state satellite peak. Panels (b)-(d) show the spectral function at times $tT_K = 0.001$, 1 and 1000, respectively. The TDNRG calculations used a discretization parameter $\Lambda = 4$, z averaging [74, 75] with $N_z = 32$ and a cutoff energy $E_{cut} = 24$.

gradually filled in by a transfer of spectral weight from higher energies [Fig. 1(c)] to form the final state Kondo resonance at long times [Fig. 1(d)]. The presence of a structure on the final state Kondo scale T_K at short times $t \to 0^+$ is understood as follows: the Fourier transform with respect to $t' = t_1 - t_2$ necessarily convolutes information about the final state at large t_1, t_2 into the spectral function at short-times t [79]. Hence, the gross features of the spectral function, even at short times $t \to 0^+$, are close to those of the final state spectral function $A(\omega, t \to \infty)$, and far from those of the initial state spectral function. Clear signatures of the latter, such as the much narrower initial state Kondo peak, only appear at negative times.

Consider now quench (B), in which the system, is switched from the mixed valence to the symmetric Kondo regime. Figures 2(a)-(b) show the overall time-dependence of the spectral function for $\omega < 0$ [Figure 2(a)] and $\omega > 0$ [Figure 2(b)]. As for quench (A), two structures associated with two energy scales are again visible at all times $t > 0$: the satellite peaks at $\omega = \varepsilon_f \approx -40 T_K$ [Figure 2(a)] and $\omega = \varepsilon_f + U \approx +40 T_K$ [Figure 2(b)] and a structure on the scale of T_K around the Fermi level [Figs. 2(a) and 2(b)]. In contrast to quench (A), the former have some non-negligible time-dependence at short positive times as can be seen in Fig. 2(c) for $tT_K = 10^{-4}$ ($t\Gamma = 10^{-3}$), where the weight of the satellite peaks has still
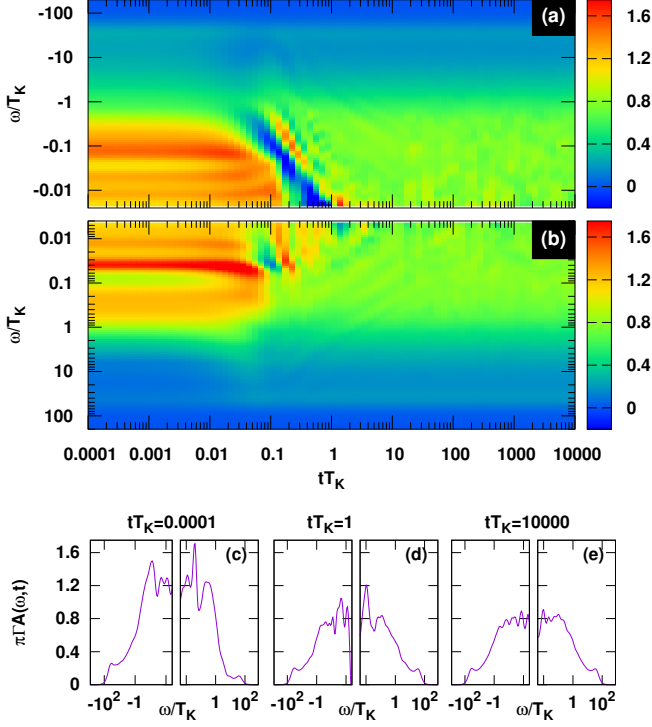
FIG. 2. Time evolution of the normalized spectral function $\pi\Gamma A(\omega, t)$ at positive times, for, (a), negative, and, (b), positive frequencies, for quench (A) from the mixed valence to the symmetric Kondo regime with $T_K = 1.0 \times 10^{-4}$. A structure on the scale of T_K evolves into the Kondo resonance at long times $t \gtrsim 1/T_K$, while structures at $\omega = \pm\varepsilon_f \approx \pm 40 T_K$, with negligible time-dependence, correspond to the final state satellite peaks. Panels (c)-(f) show the spectral function at times $tT_K = 0.0001, 1$ and 10000, respectively. TDNRG parameters: $\Lambda = 4$, z averaging with $N_z = 64$ and a cutoff energy $E_{\text{cut}} = 24$.

not equalized. This asymmetry vanishes on time scales exceeding $1/\Gamma$ [Figs. 2(d) and 2(e) for $tT_K = 1$ ($t\Gamma = 10$) and $tT_K = 10^4$ ($t\Gamma = 10^3$), respectively]. The low energy structure of width T_K, initially asymmetric and exceeding the unitary height $1/\pi\Gamma$, has significant time-dependence for $t > 0$ and evolves into the fully developed Kondo resonance at $t \gtrsim 1/T_K$ [Figs. 2(d) and 2(e)]. The deviation from the Friedel sum rule $\pi\Gamma A(\omega = 0, t \to \infty) = 1$ is comparable to that for quench (A) and reflects the incomplete thermalization due to the discrete Wilson chain used within TDNRG. The discrete Wilson chain also results in the substructures at $|\omega| \lesssim T_K$ in Figs. 2(c) and 2(d) and in the small remaining asymmetry of the fully developed Kondo resonance in Fig. 2(e).

From negative to positive times.— Figures 3(a) and 3(b) show the overall time-dependence of the spectral function for negative and positive times, respectively, for quench (A), on a *linear* frequency scale. As for positive times [Fig. 1(a) and Fig. 3(b)], low and high energy structures are visible also for negative times [Fig. 3(a)]. Moreover, it is clear from Figs. 3(a) and 3(b) that the transition from the initial to the final state spectral function occurs on different time scales for the differ-
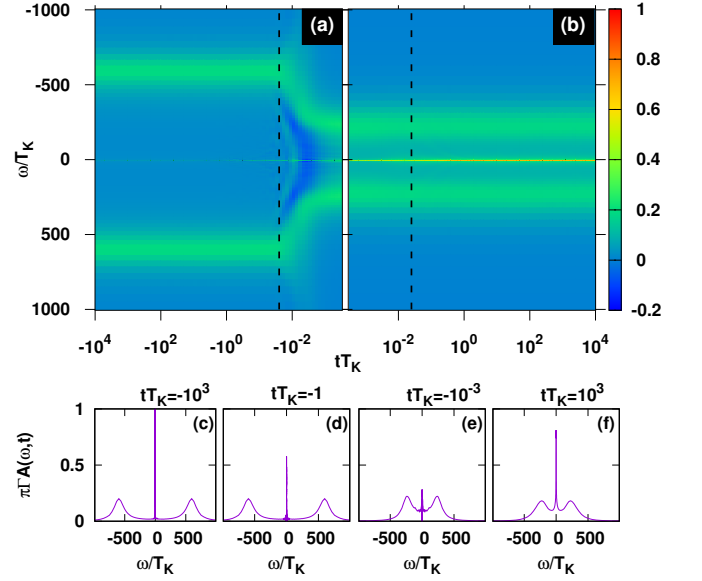

FIG. 3. $A(\omega, t)$ vs tT_K from, (a), negative, to, (b), positive times for quench (A), and on a *linear* frequency scale. Dashed lines mark $t\Gamma = \pm 1$ ($tT_K = \pm 2.5 \times 10^{-2}$). Initial state ($\omega = \pm\varepsilon_i = \pm 15\Gamma \approx \pm 600 T_K$) and final state ($\omega = \pm\varepsilon_f = \pm 6\Gamma \approx \pm 240 T_K$) satellite peaks are clearly visible, as are initial and final state Kondo resonances around $\omega = 0$. Panels (c)-(e) show the $A(\omega, t)$ at times $tT_K = -1000, -1, -0.001$ and $+1000$, respectively. TDNRG parameters as in Fig. 2.

ent structures. Consider first the high energy structures, which carry essentially all the spectral weight. Initially, these are located at $\omega = \pm\varepsilon_i \approx \pm 600 T_K$ as is clearly visible in Fig. 3(a) or in Fig. 3(c) for $tT_K = -10^3$ ($t\Gamma = -4 \times 10^4 \ll -1$). They cross over to their final state positions at $\omega = \pm\varepsilon_f = \pm 240 T_K$ when $tT_K \gtrsim -10^{-2}$ ($t\Gamma \gtrsim -0.4$) [Figs. 3(a) and 3(e)], i.e., on the charge fluctuation time scale $1/\Gamma$. This can also be seen in Figs. 3(d) and 3(e). This large shift in spectral weight from $\omega = \pm\varepsilon_i$ to $\omega = \pm\varepsilon_f$ in the time-range $-10^{-2} \lesssim tT_K \lesssim -10^{-3}$ ($-0.4 \lesssim t\Gamma \lesssim -0.04$), clearly seen in Fig. 3(a), is accompanied by small regions of negative spectral weight in this transient time range [73]. This does not violate any exact results for time-dependent, as opposed to steady-state, spectral functions, and is observed in other systems [30, 80, 81]. The spectral sum rule is satisfied analytically exactly at all times and numerically within 1% at all negative times and to higher accuracy at positive times for all quench protocols [73]. Turning now to the low energy structure, i.e., the Kondo resonance, the use of a linear frequency scale now allows the initial state Kondo resonance at $\omega = 0$ to be clearly seen in Fig. 3(a) [see also Fig. 3(c)]. This structure, of width $T_K^i \ll T_K$ at $t \to -\infty$ and satisfying the Friedel sum rule $\pi\Gamma A(\omega = 0, t \to -\infty) = 1$, gradually broadens and acquires a width of T_K at short negative times [73], and then evolves into the fully developed Kondo resonance on positive time scales $tT_K \gtrsim 1$ [Fig. 3(e)].

Even more interesting is the negative [Fig. 4(a)] to positive [Fig. 4(b)] time evolution of the spectral function upon quenching from the mixed valence to the symmetric Kondo
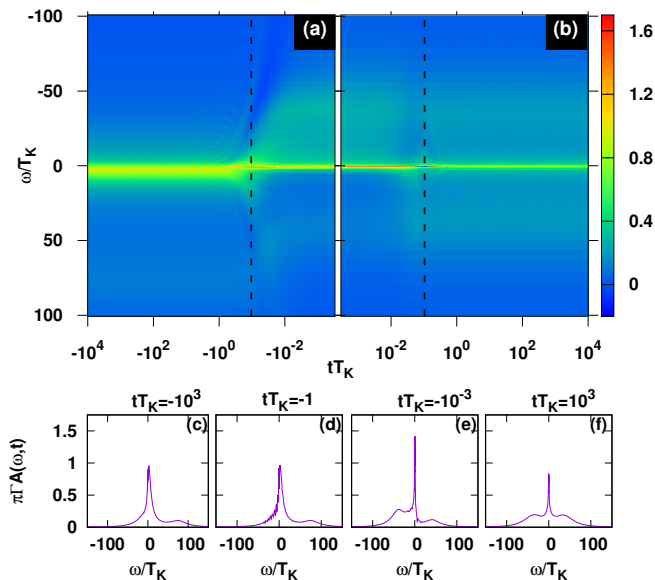
FIG. 4. $A(\omega, t)$ vs tT_K from, (a), negative, to, (b), positive times and on a *linear* frequency scale for quench (B) (from a mixed valence to a symmetric Kondo regime). Dashed lines mark $t\Gamma = \pm 1$ ($tT_K = \pm 10^{-1}$). Panels (c)-(e) show the spectral function at times $tT_K = -1000, -1, -0.001$ and $+1000$, respectively. TDNRG parameters as in Fig. 2.

regime [quench (B)]. At large negative times [Fig. 4(c)], one recovers the initial state spectral function of the mixed valence regime (with $\varepsilon_i = -\Gamma$) showing a mixed valence resonance, renormalized by many-body effects to lie close to, but just above the Fermi level $\varepsilon_i \to \tilde{\varepsilon}_i \gtrsim 0$ and satisfying the Friedel sum rule $A(0, t \to -\infty) = \sin^2(\pi n_d/2)/\pi\Gamma$ to within 3% [82] [Figs. 4(a) and 4(c), $n_d = 0.675$]. The upper satellite peak at $\omega = \varepsilon_i + U_i = 7\Gamma \approx 70 T_K$ is more clearly visible in Fig. 4(c). These peaks give rise to the final state satellite peaks at $\omega = \pm\varepsilon_f = \pm 4\Gamma \approx \pm 40 T_K$ which start to form already at negative times $tT_K \gtrsim -10^{-1}$ ($t\Gamma \gtrsim -1$), i.e., on the charge fluctuation time scale $1/\Gamma$, as for quench (A). While the positions of these peaks start to shift to their final state values at negative times $tT_K \gtrsim -10^{-1}$ ($t\Gamma \gtrsim -1$), their weights remain disparate [see Fig. 4(e)] and only equalize at $tT_K \gtrsim +10^{-1}$ ($t\Gamma \gtrsim +1$) as clearly seen in Fig. 4(b), i.e., the formation of the high energy final state satellite peaks occurs on a fast time scale $t \approx 1/\Gamma$ in the interval $-1/\Gamma \lesssim t \lesssim +1/\Gamma$ (dashed lines in Fig.4). Going into more details, we see in Figs. 4(a) and 4(c)-(e) the deconstruction of the mixed valence resonance in the time range $-1/\Gamma < t < 0$. While this resonance carries essentially all the spectral weight at $t \ll -1/\Gamma$, weight is gradually transferred to $\omega < 0$, with precursor oscillations starting at $tT_K = -1$ ($t\Gamma = -10$) [Fig. 4(d)], to form the lower final state satellite peak at $\omega = \varepsilon_f$ for $-1/\Gamma < t < 0$ [Fig. 4(e)] . Simultaneously, the mixed valence resonance narrows from its original width $\Gamma \approx 10 T_K$ and shifts towards the Fermi level to form a low energy structure on the scale of T_K [Fig. 4(e)]. The latter eventually evolves into the final state Kondo resonance

at $tT_K \gtrsim 1$. The final state spectral function is recovered in the long-time limit $tT_K \gg 1$ [Fig. 4(f)].

Conclusions.— In summary, we investigated within the TD-NRG the time evolution of the spectral function of the Anderson impurity model in the strong correlation limit. Quenching into a Kondo correlated final state, we showed that the Kondo resonance in the zero temperature spectral function only fully develops at very long times $t \gtrsim 1/T_K$, although a preformed version of it is evident even at very short times $t \to 0^+$. The latter can be used as a smoking gun signature of the transient build up of the Kondo resonance in future cold atom realizations of the Anderson impurity model [50]. The satellite peaks evolve from their initial state values at negative times on a much faster time scale $t \approx 1/\Gamma$ in the time-interval $-1/\Gamma \lesssim t \lesssim 1/\Gamma$. Our formulation of sum rule conserving two-time nonequilibrium Green functions within TDNRG, including lesser Green functions, and their explicit dependence on both times [73], yields the basic information required for applications to time-dependent quantum transport [30] and constitutes a first step towards using TDNRG as an impurity solver within nonequilibrium DMFT [41, 42, 83].

[1] A. C. Hewson, Phys. Rev. Lett. **70**, 4007 (1993).
[2] K. G. Wilson, Rev. Mod. Phys. **47**, 773 (1975).
[3] H. R. Krishna-murthy, J. W. Wilkins, and K. G. Wilson, Phys. Rev. B **21**, 1003 (1980).
[4] R. Bulla, T. A. Costi, and T. Pruschke, Rev. Mod. Phys. **80**, 395 (2008).
[5] C. Gonzalez-Buxton and K. Ingersent, Phys. Rev. B **57**, 14254 (1998).
[6] E. Gull, A. J. Millis, A. I. Lichtenstein, A. N. Rubtsov, M. Troyer, and P. Werner, Rev. Mod. Phys. **83**, 349 (2011).
[7] S. R. White, Phys. Rev. Lett. **69**, 2863 (1992).
[8] A. M. Tsvelick and P. B. Wiegmann, Advances in Physics **32**, 453 (1983).
[9] N. Andrei, "Integrable models in condensed matter physics," in *Low-Dimensional Quantum Field Theories for Condensed Matter Physicists* (World Scientific Publishing Co, 2013) pp. 457–551.
[10] R. Brako and D. Newns, Surface Science **108**, 253 (1981).
[11] H. Kasai and A. Okiji, Surface Science **183**, 147 (1987).
[12] J. Merino and J. B. Marston, Phys. Rev. B **58**, 6982 (1998).
[13] D. C. Langreth and P. Nordlander, Phys. Rev. B **43**, 2541 (1991).
[14] H. Shao, D. C. Langreth, and P. Nordlander, Phys. Rev. B **49**, 13929 (1994).
[15] H. Shao, D. C. Langreth, and P. Nordlander, Phys. Rev. B **49**, 13948 (1994).

[16] M. Pamperin, F. X. Bronold, and H. Fehske, Phys. Rev. B **91**, 035440 (2015).

[17] X. He and J. A. Yarmoff, Phys. Rev. Lett. **105**, 176806 (2010).

[18] S. Hershfield, J. H. Davies, and J. W. Wilkins, Phys. Rev. B **46**, 7046 (1992).

[19] S. Hershfield, Phys. Rev. Lett. **70**, 2134 (1993).

[20] Y. Meir, N. S. Wingreen, and P. A. Lee, Phys. Rev. Lett. **70**, 2601 (1993).

[21] C. Bruder and H. Schoeller, Phys. Rev. Lett. **72**, 1076 (1994).

[22] A. V. Kretinin, H. Shtrikman, D. Goldhaber-Gordon, M. Hanl, A. Weichselbaum, J. von Delft, T. Costi, and D. Mahalu, Phys. Rev. B **84**, 245316 (2011).

[23] A. V. Kretinin, H. Shtrikman, and D. Mahalu, Phys. Rev. B **85**, 201301 (2012).

[24] M. Pletyukhov and H. Schoeller, Phys. Rev. Lett. **108**, 260601 (2012).

[25] G. D. Scott, D. Natelson, S. Kirchner, and E. Muñoz, Phys. Rev. B **87**, 241104 (2013).

[26] P. Nordlander, M. Pustilnik, Y. Meir, N. S. Wingreen, and D. C. Langreth, Phys. Rev. Lett. **83**, 808 (1999).

[27] J. Park, A. Pasupathy, J. Goldsmith, C. Chang, Y. Yaish, J. Petta, M. Rinkoski, J. Sethna, H. Abruna, P. McEuen, and D. Ralph, Nature **417**, 722 (2002).

[28] A. Kogan, S. Amasha, and M. A. Kastner, Science **304**, 1293 (2004).

[29] B. Hemingway, S. Herbert, M. Melloch, and A. Kogan, Phys. Rev. B **90**, 125151 (2014).

[30] A.-P. Jauho, N. S. Wingreen, and Y. Meir, Phys. Rev. B **50**, 5528 (1994).

[31] D. M. Kennes, S. G. Jakobs, C. Karrasch, and V. Meden, Phys. Rev. B **85**, 085113 (2012).

[32] G. Cohen, E. Gull, D. R. Reichman, and A. J. Millis, Phys. Rev. Lett. **112**, 146802 (2014).

[33] T. L. Schmidt, P. Werner, L. Mühlbacher, and A. Komnik, Phys. Rev. B **78**, 235110 (2008).

[34] A. Dorda, M. Nuss, W. von der Linden, and E. Arrigoni, Phys. Rev. B **89**, 165105 (2014).

[35] A. Rosch, J. Paaske, J. Kroha, and P. Wölfle, Phys. Rev. Lett. **90**, 076804 (2003).

[36] A. E. Antipov, Q. Dong, and E. Gull, Phys. Rev. Lett. **116**, 036801 (2016).

[37] W. Metzner and D. Vollhardt, Phys. Rev. Lett. **62**, 324 (1989).

[38] A. Georges, G. Kotliar, W. Krauth, and M. J. Rozenberg, Rev. Mod. Phys. **68**, 13 (1996).

[39] G. Kotliar and D. Vollhardt, Physics Today **57**, 53 (2004).

[40] P. Schmidt and H. Monien, eprint arXiv:cond-mat/0202046 (2002), cond-mat/0202046.

[41] J. K. Freericks, V. M. Turkowski, and V. Zlatić, Phys. Rev. Lett. **97**, 266408 (2006).

[42] H. Aoki, N. Tsuji, M. Eckstein, M. Kollar, T. Oka, and P. Werner, Rev. Mod. Phys. **86**, 779 (2014).

[43] M. Eckstein and M. Kollar, Phys. Rev. B **78**, 205119 (2008).

[44] J. K. Freericks, H. R. Krishnamurthy, and T. Pruschke, Phys. Rev. Lett. **102**, 136401 (2009).

[45] L. Perfetti, P. A. Loukakos, M. Lisowski, U. Bovensiepen, H. Berger, S. Biermann, P. S. Cornaglia, A. Georges, and M. Wolf, Phys. Rev. Lett. **97**, 067402 (2006).

[46] P. A. Loukakos, M. Lisowski, G. Bihlmayer, S. Blügel, M. Wolf, and U. Bovensiepen, Phys. Rev. Lett. **98**, 097401 (2007).

[47] E. Iyoda and S. Ishihara, Phys. Rev. B **89**, 125126 (2014).

[48] S. Loth, M. Etzkorn, C. P. Lutz, D. M. Eigler, and A. J. Heinrich, Science **329**, 1628 (2010).

[49] Y. Nishida, Phys. Rev. Lett. **111**, 135301 (2013).

[50] J. Bauer, C. Salomon, and E. Demler, Phys. Rev. Lett. **111**, 215304 (2013).

[51] Y. Nishida, Phys. Rev. A **93**, 011606 (2016).

[52] L. Riegger, N. Darkwah Oppong, M. Höfer, D. Rio Fernandes, I. Bloch, and S. Fölling, ArXiv e-prints (2017), arXiv:1708.03810.

[53] J. Goold, T. Fogarty, N. Lo Gullo, M. Paternostro, and T. Busch, Phys. Rev. A **84**, 063632 (2011).

[54] M. Knap, A. Shashi, Y. Nishida, A. Imambekov, D. A. Abanin, and E. Demler, Phys. Rev. X **2**, 041020 (2012).

[55] M. Cetina, M. Jag, R. S. Lous, I. Fritsche, J. T. M. Walraven, R. Grimm, J. Levinsen, M. M. Parish, R. Schmidt, M. Knap, and E. Demler, Science **354**, 96 (2016).

[56] F. B. Anders and A. Schiller, Phys. Rev. Lett. **95**, 196801 (2005).

[57] F. B. Anders and A. Schiller, Phys. Rev. B **74**, 245113 (2006).

[58] F. B. Anders, Phys. Rev. Lett. **101**, 066804 (2008).

[59] F. B. Anders, Journal of Physics-Condensed Matter **20**, 195216 (2008).

[60] F. Güttge, F. B. Anders, U. Schollwöck, E. Eidelstein, and A. Schiller, Phys. Rev. B **87**, 115115 (2013).

[61] H. T. M. Nghiem and T. A. Costi, Phys. Rev. B **89**, 075118 (2014).

[62] H. T. M. Nghiem and T. A. Costi, Phys. Rev. B **90**, 035129 (2014).

[63] F. Randi, D. Fausti, and M. Eckstein, Phys. Rev. B **95**, 115132 (2017).

[64] S. Bock, A. Liluashvili, and T. Gasenzer, Phys. Rev. B **94**, 045108 (2016).

[65] D. Lobaskin and S. Kehrein, Phys. Rev. B **71**, 193303 (2005).

[66] M. Heyl and S. Kehrein, Phys. Rev. B **81**, 144301 (2010).

[67] I. Weymann, J. von Delft, and A. Weichselbaum, Phys. Rev. B **92**, 155435 (2015).

[68] The use of a discretized Wilson chain within TDNRG results, to a small degree, in incomplete thermalization at $t \to \infty$ in thermodynamic observables [57, 61, 76, 84], and in spectral functions [59, 67], but it suffices for a consistent nonperturbative picture of the overall time evolution of $A(\omega, t)$.

[69] We use the Bethe ansatz expression $T_K = \sqrt{\Gamma U/2}e^{-\pi U/8\Gamma + \pi\Gamma/2U}$ valid in the symmetric Kondo limit $U/\pi\Gamma \gg 1$ [1, 85].

[70] A. Weichselbaum and J. von Delft, Phys. Rev. Lett. **99**, 076402 (2007).

[71] R. Peters, T. Pruschke, and F. B. Anders, Phys. Rev. B **74**, 245114 (2006).

[72] T. A. Costi and V. Zlatić, Phys. Rev. B **81**, 235127 (2010).

[73] See Supplementary Material [URL] for derivations and additional results, including Ref. 86.

[74] W. C. Oliveira and L. N. Oliveira, Phys. Rev. B **49**, 11986 (1994).

[75] V. L. Campo and L. N. Oliveira, Phys. Rev. B **72**, 104432 (2005).

[76] A. Rosch, The European Physical Journal B-Condensed Matter and Complex Systems **85**, 1 (2012).

[77] R. Bulla, A. C. Hewson, and T. Pruschke, Journal of Physics: Condensed Matter **10**, 8365 (1998).

[78] E. Eidelstein, A. Schiller, F. Güttge, and F. B. Anders, Phys. Rev. B **85**, 075118 (2012).

[79] V. Turkowski and J. K. Freericks, Phys. Rev. B **71**, 085104 (2005).

[80] A. Dirks, M. Eckstein, T. Pruschke, and P. Werner, Phys. Rev. E **87**, 023305 (2013).

[81] J. K. Freericks and V. Turkowski, Phys. Rev. B **80**, 115119 (2009).

[82] T. A. Costi, J. Kroha, and P. Wölfle, Phys. Rev. B **53**, 1850

(1996).

[83] C. Gramsch, K. Balzer, M. Eckstein, and M. Kollar, Phys. Rev. B **88**, 235106 (2013).

[84] H. T. M. Nghiem, D. M. Kennes, C. Klöckner, V. Meden, and T. A. Costi, Phys. Rev. B **93**, 165130 (2016).

[85] V. Zlatić and B. Horvatić, Phys. Rev. B **28**, 6904 (1983).

[86] R. Bulla, T. A. Costi, and D. Vollhardt, Phys. Rev. B **64**, 045103 (2001).